



Radiative recombination of indirect exciton in type-II ZnSeTe/ZnSe multiple quantum wells

Chin-Hau Chia^{a,*}, Wen-Chung Fan^b, Yen-Chen Lin^b, Wu-Ching Chou^b

^a Department of Applied Physics, National University of Kaohsiung, Kaohsiung 81148, Taiwan, R.O.C

^b Department of Electrophysics, National Chiao Tung University, HsinChu 30010, Taiwan, R.O.C

ARTICLE INFO

Article history:

Received 10 November 2010

Received in revised form

28 December 2010

Accepted 31 December 2010

Available online 7 January 2011

Keywords:

ZnSeTe

Type-II quantum well

Time-resolved photoluminescence

Exciton

ABSTRACT

The tunability of the emission energy, oscillator strength and photoluminescence (PL) efficiency by varying the well thickness and excitation density was demonstrated in the ZnSe_{0.8}Te_{0.2}/ZnSe multiple quantum wells. A significant blueshift about 260 meV of the PL peak energy was observed as the well width decreased from 5 to 1 nm. An extraordinary long lifetime (300 ns) of the recombination for the widest sample was detected. The binding energy of the indirect excitons is determined as 12 meV for the thinnest sample. The reduction of PL efficiency by thermal energy is greatly suppressed by employing a high excitation power.

Crown Copyright © 2011 Published by Elsevier B.V. All rights reserved.

The ZnSe_{1-x}Te_x system has long been of interest, since it is relatively easy to obtain *n*-type ZnSe and *p*-type ZnTe. Therefore, many studies on the 3D bulk structure of ZnSe_{1-x}Te_x have been performed to understand this system [1–4]. A ZnSeTe-based light-emitting device in the blue–green spectral region has also been proposed [5]. The photoluminescence (PL) of ZnSe/ZnTe superlattice structures is attributed to isoelectronically bound excitons [5–7], instead of quantum-confined excitons. The quantum confinement effect of Te-bound excitons is only significant in an extremely thin layer [7]. However, the quantum efficiency, which is a crucial factor for optimizing light-emitting device, is not investigated. Another interesting aspect of ZnTe/ZnSe systems is the type-II band-alignment of the heterostructures [2,5–7]. Type-II quantum structures should exhibit a large tunability of emission energy and a dependence of oscillator strength on size [8]. Due to the spatial separation of electrons and holes, the radiative lifetimes for type-II quantum structures should be longer than that for the type-I case. Te-bound holes can induce a long recombination time for the excitons in ZnSeTe compound [9]. Therefore, a further lengthening of the Te-bound exciton lifetime in the type-II heterostructures is expected, to make this system more promising for optical memories [10].

In this letter, 10-period quantum-well structures consist of heavily Te-doped layers of ZnSe sandwiched between undoped ZnSe layers were studied. A significant blueshift of PL energy and

long exciton lifetimes were observed for the multiple quantum wells (MQWs). The temperature (*T*) dependence of radiative efficiency was investigated. The thermal quenching of the PL intensity was found to depend crucially on excitation power.

A set of 10-period MQWs, [ZnSe_{0.8}Te_{0.2}/ZnSe]₁₀, was grown on a GaAs (1 0 0) substrate by molecular beam epitaxy. A 1.5-μm-thick ZnSe buffer was grown before the deposition of the MQWs. The cell temperatures of Zn, Se and Te were set at 300, 170 and 290 °C, respectively. The substrate surface temperature was kept at 310 °C throughout the growth of the MQWs. The Te concentration was determined by an energy dispersive X-ray diffraction measurement using a ZnSeTe epilayer grown under the same conditions with the MQWs. The thickness of the barrier layer (ZnSe) was kept at 20 nm, whereas the well-widths (*L_w*) for the four 10-period MQWs are 1, 2, 3 and 5 nm. The excitation source for the excitation-density-dependent PL spectroscopy was a 325 nm-line of HeCd laser and the emissions were analyzed using the SPEX 1403 double grating spectrometer in conjunction with a thermoelectrically cooled photomultiplier tube. A pulsed GaN diode laser (396 nm) with duration of 50 ps and repetition rate of 2.5 MHz was used as an excitation source for the time-resolved measurement. The peak power of the pulse was estimated to be below 0.1 mW. The transients of the PL spectra were analyzed by a high-speed photomultiplier tube, followed by a personal computer plug-in time-correlated counting card. The overall time resolution of the detection system is about 300 ps.

The low-*T* PL spectra of the MQWs, pumped under an excitation power below 0.1 mW, are depicted in Fig. 1(a). The PL peak energies are about 2.13 and 2.39 eV for the MQWs with *L_w*s of 5 and 1 nm,

* Corresponding author.

E-mail address: chchia@nuk.edu.tw (C.-H. Chia).

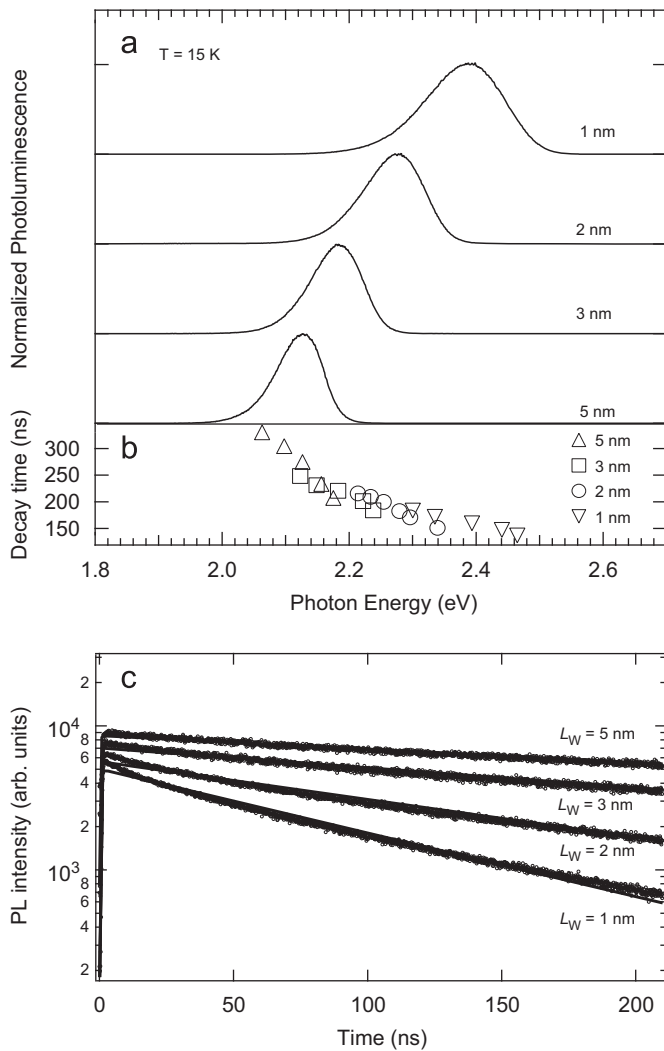


Fig. 1. (a) Low- T PL spectra of the $\text{ZnSe}_{0.8}\text{Te}_{0.2}/\text{ZnSe}$ MQWs. (b) Spectral distributions of the decay times for the $\text{ZnSe}_{0.8}\text{Te}_{0.2}/\text{ZnSe}$ MQWs at low T . (c) Evolution of PL peak intensity as a function of time.

respectively. A significant blueshift about 260 meV was observed as the L_w decreased from 5 to 1 nm. We calculated the band lineups for the MQW structures using the model–solid theory [11]. The physical parameters of the $\text{ZnSe}_{0.8}\text{Te}_{0.2}$ layers were obtained by the linear interpolation of ZnSe and ZnTe, provided in Ref. [11]. However, the $\text{ZnSe}_{1-x}\text{Te}_x$ layer should exhibit a large band-gap bowing effect, induced by an interaction between the localized Te states and degenerate Γ valence band of ZnSe [12]. Therefore, a bowing energy $bx(1-x)$ was included in the calculated valence-band energy E_v for the $\text{ZnSe}_{0.8}\text{Te}_{0.2}$. The bowing factor b was taken as 1.36 eV [13]. This yields a band lineup shown in Fig. 2(a). The E_v^{BOW} is the bowing-energy-included valence-band energy of the $\text{ZnSe}_{0.8}\text{Te}_{0.2}$. In addition to the compressive-strain-induced splitting, the heavy-hole valence-band energy E_{HH} of the $\text{ZnSe}_{0.8}\text{Te}_{0.2}$ is 0.51 eV above the E_v of ZnSe. The confinement energies of electrons and holes were then calculated by a simple square potential model. The effective masses of ZnSe and ZnTe are $m_e/m_0(\text{ZnSe})=0.145$, $m_h/m_0(\text{ZnSe})=0.49$ and $m_e/m_0(\text{ZnTe})=0.12$, $m_h/m_0(\text{ZnTe})=0.6$ [13]. The effective masses of electrons and holes in the ternary alloy $\text{ZnSe}_{0.8}\text{Te}_{0.2}$ are obtained by linear interpolation. Since the holes in the $\text{ZnSe}_{0.8}\text{Te}_{0.2}$ layer are isoelectronically trapped by the Te-clusters [1] (denotes as Te-trap level (dotted line) in Fig. 2(a)), the calculated transition energy was given by $E_g(\text{ZnSe}) + E_h + E_e - \Delta E_v - E_{\text{IC}}$. Here, E_h and E_e are the confinement energy of the holes in the $\text{ZnSe}_{1-x}\text{Te}_x$ layers and the electrons in the ZnSe layers, respectively. The isoelectronic-trapped energy E_{IC} is taken as 200 meV, which is reasonable for $x=0.2$ [14]. The results are shown in Fig. 2(b). For comparison, the calculated transition energy for the unstrained MQWs (dashed line) was also given. Obviously, the calculated transition energy for the strained case matched more to the experimental PL peak energies, compared to that for the unstrained case. However, the calculated values gradually deviated from the experimental values as the L_w decreased. This might be induced by a diffusion of Te-atoms or Se-atoms into the adjacent layers [2], leading to a great modification of band profiles at the interface. Qualitatively, this effect would cause an increase in the transition energy, resulting from the reduction in the minimum of the binding potential. [15].

We also measured the spectral distribution of PL decay time (τ_{PL}), as shown in Fig. 1(b). Fig. 1(c) shows the evolution of PL peak intensity as a function of time. The decay curves of the PL can be roughly fitted by a single time constant using $I_{\text{PL}}(t) = I_0 \exp(-t/\tau_{\text{PL}})$.

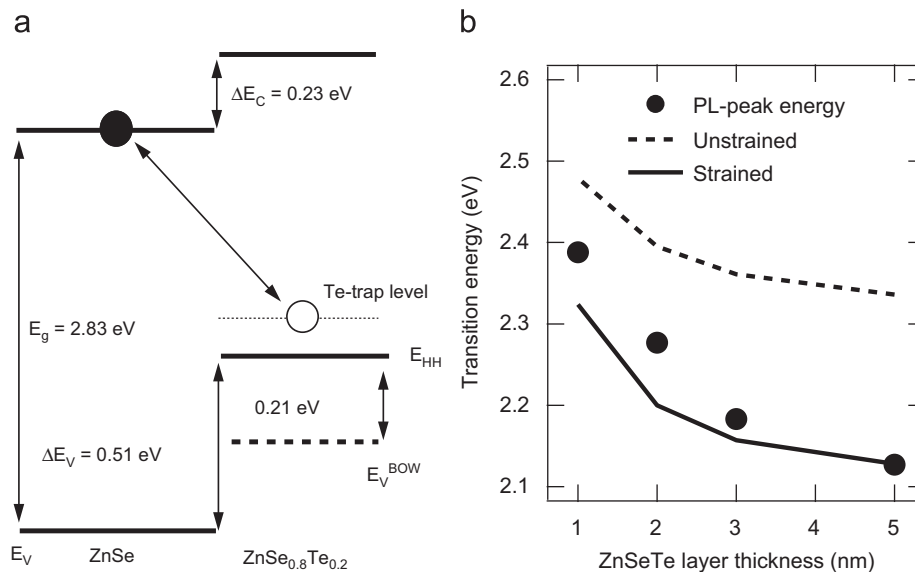


Fig. 2. (a) Calculated band lineup for the $\text{ZnSe}_{0.8}\text{Te}_{0.2}/\text{ZnSe}$ MQWs. (b) L_w dependence of PL peak energies (solid circles). Solid and dashed lines represent the calculated transition energies for the strained and unstrained case, respectively.

The enhancement of τ_{PL} was observed as L_w increased. This is not surprising since the electron–hole wavefunction-overlap is a decisive factor for the observed decay times in the type-II structures. In other words, the increase in L_w results in the reduction in wavefunction-overlap between the spatially separated electrons and holes, thus, a suppression of decay rate. Moreover, the long lifetimes (above 150 ns) of Te-bound excitons are also a signature for type-II recombination. A decay time of 30 ns has been reported for a bulk $\text{ZnSe}_{1-x}\text{Te}_x$ with $x=0.12$ [9]. The reason for the long lifetime of $\text{ZnSe}_{1-x}\text{Te}_x$ system even for the bulk structure is the suppression of hole wavefunction by Te-clusters [16], and hence a reduction of the oscillator strength of excitons. Further enhancement of decay times in the QW structures, therefore, can be attributed to a further spatial separation of the carriers confined in different layers.

We further confirm the type-II nature of the emissions in the MQWs. The evolution of PL peak energy as a function of excitation power for the typical MQW ($L_w=3$ nm) is shown in Fig. 3(a). There is a significant blueshift for the PL bands as the excitation power increases. This phenomenon is interpreted as being caused by the carrier-induced band-bending effect at the heterointerfaces [2,17]. As the excitation density increases, the increase in

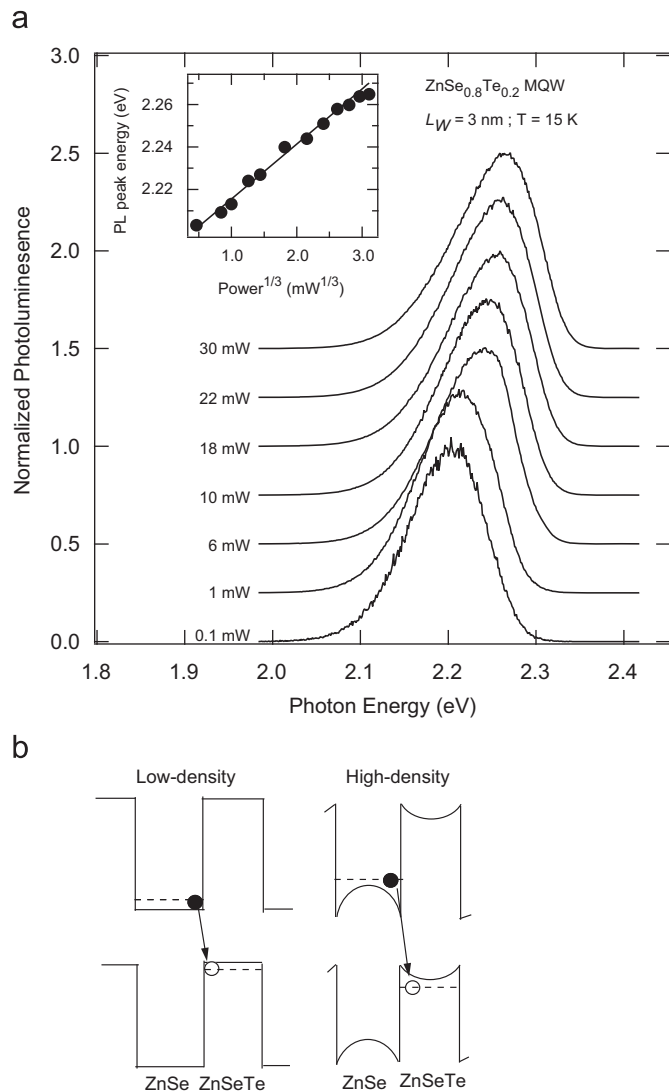


Fig. 3. (a) Evolution of PL spectra as a function of excitation power for sample with L_w of 3 nm. Inset shows the cube root dependence of the PL peak energy against the excitation power. (b) Recombination processes under low-density case and high-density case. Band-bending at the interfaces is induced by carriers under high-density case.

population of spatially confined electron–hole pairs strengthens the band-bending effect at the heterointerfaces, as shown in Fig. 3(b). The sheet concentration generated at the heterointerfaces by an excitation density I_{exc} is characterized by $n_s = I_{\text{exc}} \alpha d / \gamma \hbar \nu$ [18]. Here, α is the absorption coefficient, d is the depletion layer thickness, ν is the frequency of laser light and γ is the radiative recombination coefficient. The localized electrons and holes form a charged plane with an electric field $F = 2\pi e n_s / \epsilon_0$. This yields the quantized energy $E \propto F^{2/3} \propto I_{\text{exc}}^{1/3}$ in the triangular potential well [2,15–17]. This is in good agreement with our experimental data (inset of Fig. 3). Hence, the PL of the $\text{ZnSe}_{0.8}\text{Te}_{0.2}/\text{ZnSe}$ MQWs is attributable to the radiative recombination between holes that are localized in the $\text{ZnSe}_{0.8}\text{Te}_{0.2}$ layers and electrons in the ZnSe barrier region.

T -dependent PL efficiencies of the $\text{ZnSe}_{0.8}\text{Te}_{0.2}/\text{ZnSe}$ MQWs were investigated by both the T -dependent PL intensity (I_{PL}) and lifetimes. The evolution of τ_{PL} (solid circles) measured at the PL peak energy as a function of T for the sample with $L_w=1$ nm, is shown in Fig. 4(a). The lifetime increases initially from low T to 100 K (from 160 to 184 ns), and decreases monotonically above 120 K. We estimated the radiative (τ_r) and nonradiative (τ_{nr}) lifetimes by a combined analysis of T -dependent I_{PL} and τ_{PL} [18]. Considering only radiative and nonradiative recombination processes, the internal radiative yield, $\eta = \tau_{\text{nr}} / (\tau_{\text{nr}} + \tau_r)$, rules the variation of I_{PL} versus T . Since the measured τ_{PL} can be given by $\tau_{\text{PL}}^{-1} = \tau_r^{-1} + \tau_{\text{nr}}^{-1}$, we can obtain the radiative lifetime as $\tau_r = \tau_{\text{PL}} / \eta$ by assuming η to be unity at low temperature (30 K). The assumption is reasonable because high efficiency of radiative recombination is possible at low T , due to the suppression of the migration process of excitons to the non-radiative centers [9]. The τ_{nr} is a monotonically decreasing function of T and becomes shorter than the τ_r after $T=120$ K. This indicates that the nonradiative recombination process dominates the PL after

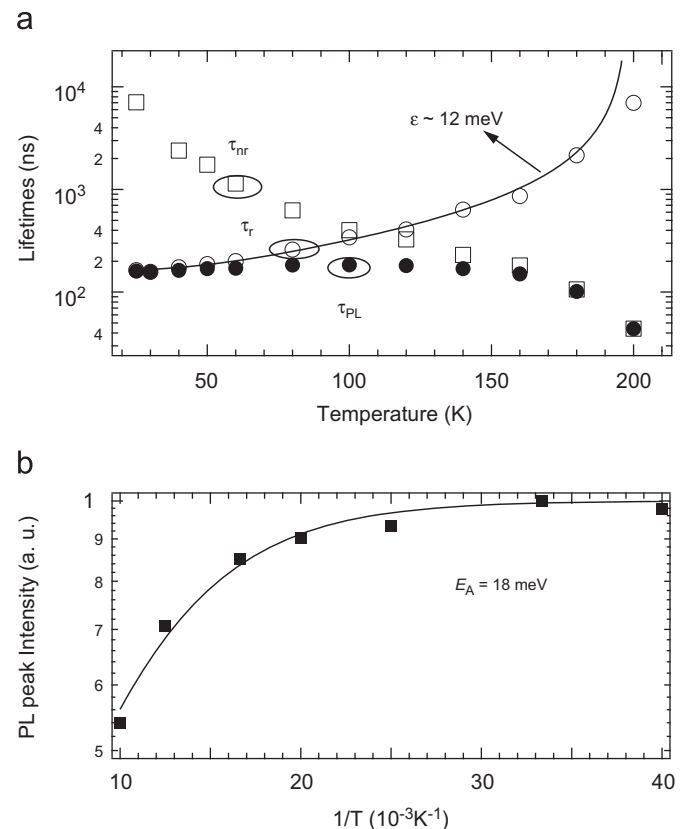


Fig. 4. (a) T dependence of τ_{PL} (solid circles), τ_r (open circles), τ_{nr} (open squares). The solid line is the fit of τ_r to $\tau_r(T) = \tau_r(0) / [1 - C \exp(-\epsilon/k_B T)]$ which yields a characteristic energy of 12 meV. (b) Arrhenius plot of the normalized PL peak intensity.

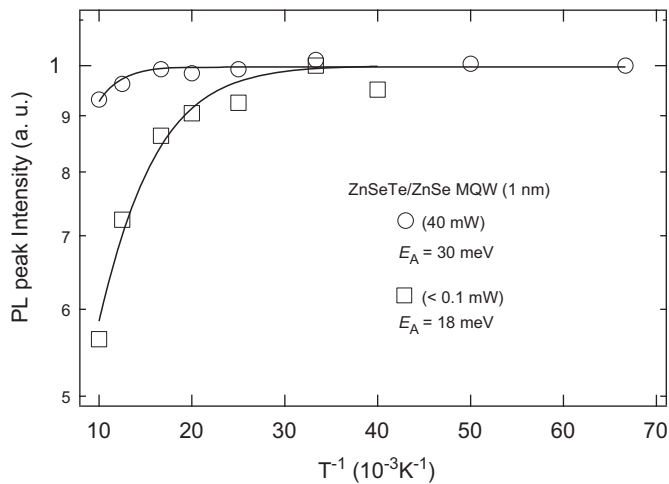


Fig. 5. T dependence of the normalized PL peak intensities for $\text{ZnSe}_{0.8}\text{Te}_{0.2}/\text{ZnSe}$ MQW ($L_w=1$ nm), under excitation power of 40 mW (circles) and below 0.1 mW (squares). The obtained activation energies are listed.

$T=120$ K. An enhancement of τ_r can be understood for isoelectronically bound exciton in type-II quantum structures, as a consequence of ionization of weakly bound electrons from the strongly localized holes. Therefore, the T dependence of τ_r can be fitted with the formula [3]: $\tau_r(T)=\tau_r(0)/[1-C\exp(-\varepsilon/k_B T)]$. Here, $\tau_r(0)$ is the radiative time at low T limit, C is a constant and ε is a characteristic energy that is of the order of the electron–hole binding energy. The best fit yields a characteristic energy of 12 meV for the binding of indirect excitons. Such a low exciton binding energy (E_b) is expected for type-II MQW structures due to the spatial separation of electrons and holes. Fig. 4(b) shows the Arrhenius plot of the normalized PL peak intensity for the same sample. The T dependence of the I_{PL} was fitted by the following equation: $I_{\text{PL}}(T)=I(0)/[1+C_A\exp(-E_A/k_B T)]$ [19]. Here, $I(0)$ is the PL intensity at 0 K. C_A is fitting constant and k_B is the Boltzmann constant. We fitted the experimental values for the T range where the excitons are not totally dissociated (below 100 K). The obtained activation energy E_A (18 meV) is comparable to E_b obtained above.

In Fig. 5, the T -dependences of I_{PL} ($L_w=1$ nm) under a pumping power of 40 mW and below 0.1 mW, are shown. The obtained value of E_A , which corresponds to the exciton binding energy, is approximately twice in the former case, compared to that of the latter. As the excitation density increases, the electric field induces further band-bending at the heterointerfaces. This causes a strong modification of the envelope functions of electrons and holes [20]. Therefore, the overlap of the electron- and hole-wavefunctions increases, resulting in a stronger bound electron–hole pairs. Indeed, a shortening of 3 orders of magnitude for the recombination lifetimes of ZnSe/BeTe superlattices under high excitation has been reported [20]. We also note that the PL efficiency retains well for the high excitation case. A decrease in only about an order of magnitude in the I_{PL} was found from low T

to 300 K. On the contrary, the PL quenches at least 2 orders of magnitude for the weak excitation case and hard to be detectable at RT. The indirect-exciton recombination rate enhances under a high excitation density, based on the aforementioned band-bending model. The effect plays an important role in the observed high emission efficiency.

In conclusion, the tunability of the emission energy, oscillator strength and PL efficiency by varying the well thickness and excitation density was demonstrated in the strained $\text{ZnSe}_{0.8}\text{Te}_{0.2}/\text{ZnSe}$ MQWs. The type-II nature of the recombination was confirmed. An extraordinary long lifetime of the MQW system was detected. Also, the binding energy of the indirect excitons is determined as 12 meV for the thinnest sample. A reduction in PL efficiency was found to be greatly suppressed by employing a high excitation power.

Acknowledgement

This work was supported by the MOE-ATU and the National Science Council under the grant number of NSC 95-2112-M-009 -047.

References

- [1] C.S. Yang, D.Y. Hong, C.Y. Lin, W.C. Chou, C.S. Ro, W.Y. Uen, W.H. Lan, S.L. Tu, J. Appl. Phys. 83 (1998) 2555.
- [2] Y. Gu, Igor L. Kuskovsky, M. van der Voort, G.F. Neumark, X. Zhou, M.C. Tamargo, Phys. Rev. B 71 (2005) 045340.
- [3] D. Lee, A. Mysyrowicz, A.V. Nurmikko, B.J. Fitzpatrick, Phys. Rev. Lett. 58 (1987) 1475.
- [4] A. Muller, P. Bianucci, C. Piermarocchi, M. Fornari, I.C. Robin, R. André, C.K. Shih, Phys. Rev. B 73 (2006) R081306.
- [5] H.C. Lee, T. Abe, Z.M. Aung, M. Adachi, T. Shirai, H. Yamada, S. Kuroda, K. Maruyama, H. Kasada, K. Ando, J. Cryst. Growth 214/215 (2000) 1096.
- [6] K. Suzuki, U. Neukirch, J. Gutowski, N. Takojima, T. Sawada, K. Imai, J. Cryst. Growth 184/185 (1998) 882.
- [7] C.S. Yang, C.C. Cheng, M.C. Kuo, P.Y. Tseng, J.L. Shen, J. Lee, W.C. Chou, S. Jeng, C.Y. Lai, T.M. Hsu, J.J. Chyi, Thin Solid Films 429 (2003) 243.
- [8] U.E.H. Laheld, F.B. Pederson, P.C. Hemmer, Phys. Rev. B 52 (1995) 2697.
- [9] A. Reznitsky, S. Permogorov, S. Verbin, A. Naumov, Yu. Korostelin, V. Novozhilov, S. Prokov'ev, Solid State Commun. 52 (1984) 13.
- [10] S. Muto, Jpn. J. Appl. Phys. 34 (Part 2) (1995) L210.
- [11] Chris G. Van de Walle, Phys. Rev. B 39 (1989) 1871.
- [12] J. Wu, W. Walukiewicz, K.M. Yu, J.W. Ager III, E.E. Heller, I. Miotkowski, A.K. Ramdas, Ching-Hua Su, I.K. Sou, R.C.C. Perera, J.D. Denlinger, Phys. Rev. B 67 (2003) 035207.
- [13] Maria C. Tamargo, II–VI Semiconductor Materials And Their Applications, Taylor & Francis, New York, 2002, p. 113–171.
- [14] M.J.S. Brasil, R.E. Nahory, F.S. Turco-Sandroff, H.L. Gilchrist, R.J. Martin, Appl. Phys. Lett. 58 (1991) 2509.
- [15] F. Hatami, M. Grundmann, N.N. Ledentsov, F. Heinrichsdorff, R. Heitz, J. Böhrer, D. Bimberg, S.S. Ruvimov, P. Werner, V.M. Ustinov, P.S. Kop'ev, Zh.I. Alferov, Phys. Rev. B 57 (1998) 4635.
- [16] Q. Fu, D. Lee, A.V. Nurmikko, L.A. Kolodziejski, R.L. Gunshor, Phys. Rev. B 39 (1989) 3173.
- [17] N.N. Ledentsov, J. Böhrer, M. Beer, F. Heinrichsdorff, M. Grundmann, D. Bimberg, S.V. Ivanov, B. Ya, S.V. Meltser, I.N. Shaposhnikov, N.N. Yassievich, P.S. Faleev, Kop'ev, Zh.I. Alferov, Phys. Rev. B 52 (1995) 14058.
- [18] J. Böhrer, A. Krost, R. Heitz, F. Heinrichsdorff, L. Eckey, D. Bimberg, H. Cerva, Appl. Phys. Lett. 68 (1996) 1072.
- [19] K. Suzuki, R.A. Hogg, Y. Arakawa, J. Appl. Phys. 85 (1999) 8349.
- [20] A.A. Maksimov, S.V. Zaitsev, I.I. Tartakovskii, V.D. Kulakovskii, D.R. Yakovlev, W. Ossau, M. Keim, G. Reuscher, A. Waag, G. Landwehr, Appl. Phys. Lett. 75 (1999) 1231.